Effect of coupling in the $^{28}Si + ^{154}Sm$ reaction studied by quasi-elastic scattering

Gurpreet Kaur,[1,*] B. R. Behera,[1,†] A. Jhingan,[2] B. K. Nayak,[3] R. Dubey,[2] Priya Sharma,[1] Meenu Thakur,[1] Ruchi Mahajan,[1] N. Saneesh,[2] Tathagata Banerjee,[2] Khushboo,[4] A. Kumar,[1] S. Mandal,[4] A. Saxena,[3] P. Sugathan,[2] and N. Rowley[5]

[1]*Department of Physics, Panjab University, Chandigarh 160014, India*

[2]*Inter-University Accelerator Centre, Aruna Asaf Ali Marg, New Delhi 110067, India*

[3]*Nuclear Physics Division, Bhabha Atomic Research Centre, Mumbai 400085, India*

[4]*Department of Physics and Astrophysics, Delhi University, New Delhi 110067, India*

[5]*Institut de Physique Nucléaire, UMR 8608, CNRS-IN2P3, and Université de Paris Sud, 91406 Orsay Cedex, France*

(Received 23 April 2016; revised manuscript received 3 July 2016; published 20 September 2016)

The study of the coupling to collective states of the ^{28}Si projectile and ^{154}Sm target in fusion mechanism is reported. Understanding such couplings is important as they influence the barrier height and the formation probability of the compound nuclei, which in turn may be related to the synthesis of superheavy elements in heavier systems. In the present work, before performing the coupled-channel calculations, we wish to obtain an experimental signature of coupling to projectile and target excitation through barrier distribution (BD) study. To this end, the BDs of the $^{28}Si + ^{154}Sm$ and $^{16}O + ^{154}Sm$ systems have been compared using existing fusion data, scaled to compensate for the differences between the nominal Coulomb barriers and the respective coupling strengths. However, the large error bars on the high-energy side of the fusion BD prevent any definite identification of such signatures. We have, therefore, performed a quasi-elastic (QE) scattering experiment for the heavier $^{28}Si + ^{154}Sm$ system and compared its results with existing QE data for the ^{16}O projectile. Since QE BDs are precise at higher energies, the comparison has shown that the BD of $^{28}Si + ^{154}Sm$ is similar to that of $^{16}O + ^{154}Sm$ to a large extent except for a peaklike structure on the higher energy side. The similarity shows that the ^{154}Sm deformation plays a major role in the fusion mechanism of $^{28}Si + ^{154}Sm$ system. The peaklike structure is attributed to ^{28}Si excitation. In contrast with previous studies, it is found that a coupled-channel calculation with vibrational coupling to the first 2^+ state of ^{28}Si reproduces this structure rather well. However, an almost identical result is found with the rotational coupling scheme if one considers the large positive hexadecapole deformation of the projectile. A value around that given by Möller and Nix ($\beta_4 \approx 0.25$) leads to a strong cancellation in the re-orientation term that couples the 2^+ state back to itself, making that state look vibrational in this process. Thus, unlike the existing fusion data, our new QE results contain subtle details about the fusion mechanism of $^{28}Si + ^{154}Sm$ system. They even show a sensitivity to the ^{28}Si hexadecapole deformation and hence may be capable of giving a physically reasonable estimate for β_4 in an indirect way.

DOI: 10.1103/PhysRevC.94.034613

I. INTRODUCTION

Many nuclei that possess collective states can be categorized as vibrational or rotational, depending principally upon the energy spacing of their various excited states. The influence of these states on the fusion mechanism is usually studied through a coupled-channel approach with coupling schemes based on harmonic vibrations for spherical nuclei or on a rigid-rotor model for statically deformed nuclei [1–3]. In such an approach, the energy of the first excited state and its coupling to the ground state are obtained from the experimental data, with the latter from the relevant transition probability $B(E\lambda)$, which can be related to a nuclear deformation parameter. For second and higher excited states, excitation energies and couplings are generally taken as those obtained within the appropriate idealized coupling scheme. Clearly this approach, generating fusion excitation function, should work well for systems involving good rotational and vibrational nuclei.

Generally, of course, nuclei do not possess such pure collective structures. Even for nuclei such as ^{58}Ni whose low-lying states do display reasonably good vibrational energies, deviations from harmonicity can already be seen in the experimental fusion barrier distribution (BD) [4]. In the present case of ^{28}Si, the 4^+ state energy (at 4.62 MeV) lies approximately halfway between the vibrational estimate ($2 \times 1.78 = 3.56$ MeV) and the rotational value ($3.33 \times 1.78 = 5.93$ MeV), based on the experimental 2^+ state energy of 1.78 MeV. So from this consideration, it is not clear which of the coupling schemes (vibrational or rotational) is more appropriate for ^{28}Si. In the literature, coupling to rotational excitation appears to explain the fusion data with spherical and near-spherical target nuclei such as ^{120}Sn, ^{100}Mo, and ^{92}Zr [5–11], but it is worth noting that Newton *et al.* [5] have found that a vibrational interaction gives a better representation of their experimental data with a ^{92}Zr target. However, earlier experiments using the scattering of electrons [12] or lighter hadrons (protons, neutrons, and α particles [13–15]) can all be fitted using a rotational coupling scheme, with the ^{28}Si *target* possessing both quadrupole (oblate) and hexadecapole (positive) deformations, although there are discrepancies in its estimated hexadecapole deformation parameter (β_4).

*Present address: Department of Physics, Akal University, Talwandi Sabo 151302, India; gkaur.phy@gmail.com

†Corresponding author: bivash@pu.ac.in

Usually, the energy levels and nuclear structure information are obtained through spectroscopic studies. Alternatively, during fusion the nuclear intrinsic properties get coupled to the internuclear distance and hence leave their fingerprint in the fusion excitation function. Hence the fusion excitation function can be considered as a different route to gain the nuclear information. Furthermore, the fusion BD can also be extracted experimentally from the fusion excitation function $\sigma_{\rm fus}(E)$ by taking the second derivative of the product $E\sigma_{\rm fus}(E)$ with respect to the center-of-mass energy E, that is, $d^2(E\sigma_{\rm fus})/dE^2$. It is much easier to see the detailed effects of the coupling in the second derivative, i.e., BD, than in an exponentially changing fusion excitation function though, of course, the same information is carried in both. Thus the fusion BD, being more useful than fusion excitation function, has opened up the possibility of using the heavy-ion fusion reaction to investigate the nuclear intrinsic degrees of freedom of interacting nuclei [16]. Earlier studies have shown that the structural properties obtained from BD studies are in agreement with the spectroscopic studies; e.g., Leigh *et al.* [17] have shown the quadrupole deformation of ^{154}Sm using fusion BD studies for the ^{16}O + ^{154}Sm system. A similar study [18] has shown the effects of excitation of the collective single phonon states in ^{148}Sm for the ^{16}O + ^{148}Sm system. Although β_4 is difficult to extract experimentally, the differences in experimental fusion BDs of ^{16}O + ^{186}W and ^{16}O + ^{154}Sm [18] reveal that fusion reactions are very sensitive not only to β_2 but also to β_4 of the target nucleus. Even though the information obtained will be a model-dependent estimation, this methodology may be of significant importance to study the radioactive nuclei where thorough spectroscopic study is difficult [19].

As mentioned, the experimental data for fusion studies are already available for the interaction of ^{28}Si with spherical and near-spherical targets. Similar studies with deformed targets are scarce; however, they are significantly important due to their association with the synthesis of superheavy elements (SHEs) where deformed actinide targets are used. Synthesis of SHEs with deformed targets are interesting as the orientation of the deformed target may significantly affect the barrier height, which in turn may influence the fusion probability or formation of SHEs. In the future, we are planning to do a series of experiments on heavy systems that lead to SHEs using deformed actinide targets. Prior to that we wish to study a lighter target ^{154}Sm having similar collective states as that of deformed actinides. Apart from shedding light on the role of coupling to target deformation, the BD study for the ^{28}Si + ^{154}Sm system would help us in understanding the relative role of projectile excitation in the presence of a deformed target. However, to date, only one study has been performed for the fusion of ^{28}Si with a deformed target ^{154}Sm [20], where the fusion excitation function alone is discussed. Instead of performing coupled-channels calculations for expected excitation of ^{28}Si (due to vibrational correlations with its ground-state rotational bands, which gives better representation of its experimental energy spectrum [21]), we first approach to obtain the signature of the excitation of ^{28}Si directly from the existing experimental data. To do this, we start by making a comparison of existing fusion data on the ^{16}O + ^{154}Sm and ^{28}Si + ^{154}Sm systems. Both of these systems have the same target nucleus and thus the same target deformation. Moreover, the ^{16}O projectile can effectively be considered as inert, since its strong octupole state (3^- at 6.1 MeV) essentially shifts the fusion barrier to lower energy without significantly affecting its shape [22]. Thus, any differences between the fusion excitation functions and BDs for the ^{16}O + ^{154}Sm and ^{28}Si + ^{154}Sm systems should elucidate the coupling to the ^{28}Si projectile. Unfortunately, in the comparison we find that above Coulomb barrier the large error bars in the BD prevent us from drawing any definite conclusion. It is clear that such a comparison needs more precise data for the ^{28}Si + ^{154}Sm system in the energy region where the ^{28}Si couplings play a role. So, new quasi-elastic (QE) data are measured for this system, and a comparison is performed between our newly obtained data and earlier QE scattering data for the ^{16}O + ^{154}Sm system [23]. Hence, the aim of this article is twofold: to extract the BD for ^{28}Si + ^{154}Sm system from QE scattering data and to understand the role of coupling to ^{28}Si projectile and ^{154}Sm target excitation in fusion process.

The article is organized as follows. In Sec. II, the comparison of the fusion excitation functions and corresponding BDs of the above two systems is presented. For the new QE measurements, experimental details and data reduction are given in Sec. III. Results of our analyses and a detailed discussion are given in Sec. IV. A summary and conclusion are presented in the last section.

II. COMPARISON OF FUSION DATA

The experimental fusion data for ^{16}O + ^{154}Sm and ^{28}Si + ^{154}Sm system are available in Refs. [16,18] and Ref. [20], respectively. To observe the influence of coupling during fusion of ^{28}Si with the ^{154}Sm target, we compared these two sets of data. To facilitate comparison, the difference in Coulomb barriers was removed by shifting the energy of the two systems by their nominal barrier heights $V_{\rm B}$, that is, by using the energy variable $(E_{\rm c.m.} - V_{\rm B})$. The nominal barriers were assumed to take their Bass model values [24]. The experimental fusion cross sections were also normalized by $\pi R_{\rm B}^2$, where $R_{\rm B}$ is the position of the Bass barrier. Figures 1(a) and 1(b) show the comparison of the fusion excitation functions and their BDs, respectively, after the above scalings. An enhancement in the fusion cross section for the ^{28}Si system with respect to that for ^{16}O can be observed in Fig. 1(a). This is accompanied by a widening of the BD, and it can be seen in Fig. 1(b) that the ^{28}Si data have a larger spread than those for ^{16}O. We shall see below that this is not due to couplings to ^{28}Si but merely due to the fact that the larger charge of this nucleus causes the barrier to occur closer to the target, in a region where coupling to the target deformation is stronger.

It is well known that the width of the BD depends up on the coupling strength. Furthermore, the coupling strength is proportional to $Z_{\rm p}Z_{\rm t}\beta$, where $Z_{\rm p}$ and $Z_{\rm t}$ are the charges of the projectile and target, respectively, and β is some average deformation parameter for the system. Although in the present study $Z_{\rm t}$ and the target contribution to β are the same for the two systems considered for comparison, the overall strength of coupling to the target differs for ^{28}Si and

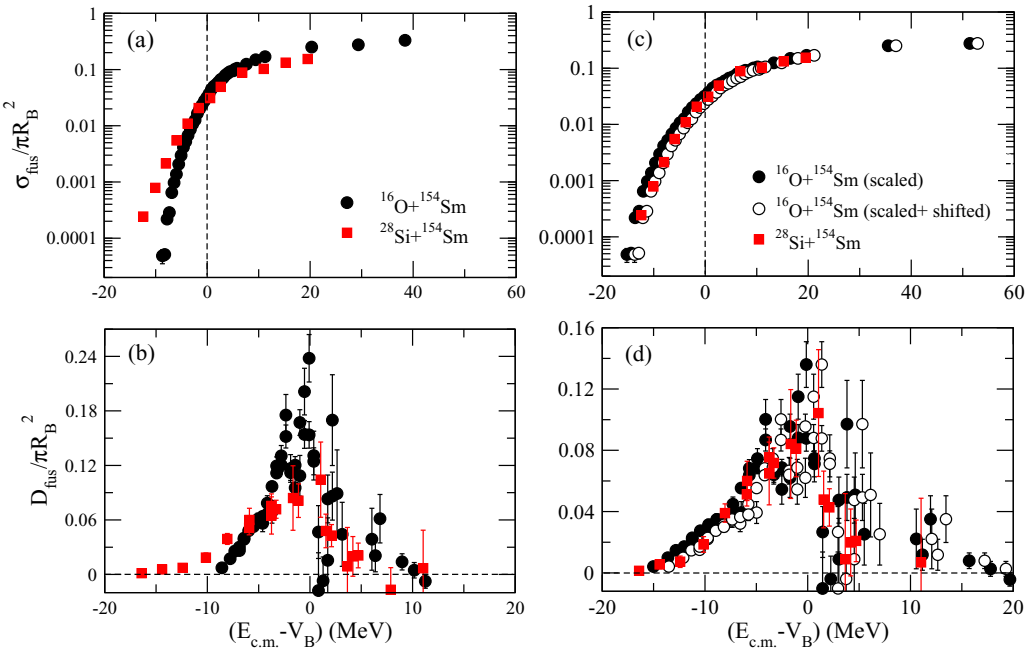

FIG. 1. Comparison of experimental fusion excitation functions (upper panels) and fusion barrier distributions (lower panels) for the systems ^{16}O + ^{154}Sm and ^{28}Si + ^{154}Sm. Left-hand plots (a) and (b) are before scaling whereas the right-hand plots (c) and (d) show the comparison after scaling the ^{16}O + ^{154}Sm data. In the right-hand plots an additional shift of 1.5 MeV for the ^{16}O + ^{154}Sm system is seen to improve the overlap of the two data sets (see text).

^{16}O projectiles. The difference is simply due to the different barrier positions produced by the different projectile charges Z_p. To remove this difference, the energy variable $(E_{c.m.} - V_B)$ for the ^{16}O + ^{154}Sm system was simply scaled by the factor $Z(^{28}\text{Si})/Z(^{16}\text{O})$. A reciprocal scaling of the ordinate axis was also performed in order to maintain the normalization of the fusion BDs. Thus this scaling facilitates a comparison of the excitation function and BD shape of two systems with elimination of differences due to projectile charge. To our knowledge, no previous study has performed these scalings, which provide insights into the relative couplings of different projectiles. This method is, of course, all the more powerful when, as here, one of the projectiles is effectively inert.

After scaling, the fusion excitation function and BDs for the two systems overlap rather well, as shown in Figs. 1(c) and 1(d), respectively, apart from an energy shift of around 1.5 MeV for the ^{16}O + ^{154}Sm system. As noted above, such a shift is indeed expected due to the strong, high-energy octupole state of ^{16}O [22]. Thus, the scaled excitation functions and BDs were shifted by a further 1.5 MeV to compensate for this. Figures 1(c) and 1(d) show the fusion excitation functions and BDs before and after this energy shift.

The ultimate, strong similarity of the scaled excitation functions and BDs for these two systems lead us to conclude that the ^{154}Sm couplings do indeed dominate these reactions. Any qualitative differences due to the couplings to the different projectiles should, though, have shown up in this comparison. However, it is clear from Fig. 1(d) that any small differences in the BDs on the high-energy side of the distribution will not be apparent due to the large error bars and an obvious gap in the data. We shall see below that this is precisely the energy region where the coupling to ^{28}Si manifests itself.

It is well established that channel couplings also affect the scattering process and the nuclear structure information can also be obtained from QE scattering cross sections at large backward angles and the corresponding BD. Indeed, this technique even allows the study of very heavy systems leading to the creation of superheavy compound nuclei where fission and quasifission dominate and identification of fusion becomes difficult. Although the precision of the fusion data could be improved, QE scattering is more appropriate for the present study since it automatically generates BDs with a smaller uncertainty in the high-energy region [25], the region of our interest. Therefore, in order to take advantage of this fact, we planned to perform the QE measurements for the ^{28}Si + ^{154}Sm system. Furthermore, for the system such as ^{28}Si + ^{154}Sm within the considered energy range, the probability of the processes, where incident flux may go apart from fusion and QE, such as deep inelastic collisions, quasifission, or noncompound fission, is negligible. Hence, the QE BD will indeed be similar to that for fusion, although the former may be somewhat smeared.

III. QE MEASUREMENTS

A. Experimental details

The experiment was carried out in the General Purpose Scattering Chamber (GPSC) facility using a ^{28}Si beam as a projectile from the 15UD Pelletron accelerator at IUAC, New Delhi. A target of ^{154}Sm (typical thickness $\approx$180 μ g/cm^2, enriched to 98.89%), sandwiched between capping ($\approx$10 μ g/cm^2) and backing ($\approx$25 μ g/cm^2) of carbon, was used. The incident energy was varied from 90.0 MeV (25% below barrier) to 135.0 MeV (11% above barrier). For

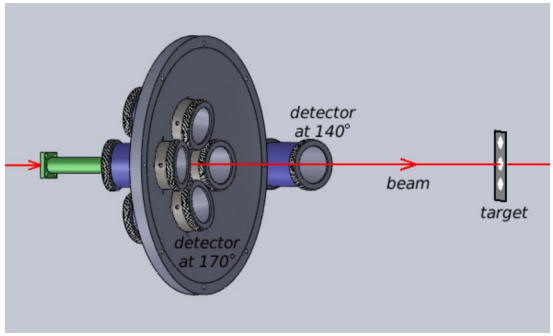

FIG. 2. Experimental setup for quasi-elastic measurements at two large backward angles, $\theta_{\rm lab} = 170^\circ$ and 140°, for the ^{28}Si + ^{154}Sm system.

a good precision of the BD measurement, the beam energy was changed in steps of 2 MeV. Below the barrier, due to high statistics, a few data points with 1 MeV energy steps were also collected. The bombarding energies were corrected for energy loss in half the target thickness, with energy loss ranging from 0.42 to 0.49 MeV for ^{28}Si. The QE measurements were performed employing hybrid telescope detectors comprising of ΔE and E detectors. The ΔE detectors were gas ionization chambers, each with active length of 18 mm, and they were operated at 90 mbar of isobutane gas. The E detectors were passivated implanted planar silicon (PIPS) detectors 300 μm thick, which were sufficient to completely stop the projectilelike (^{28}Si) particles with residual energies ranging from ≈70 to 110 MeV corresponding to scattering at different angles. The defining apertures of all the telescopes were 7 mm with an angular opening of 1.5°.

Four telescope detectors, two of them in plane and another two out of plane, each at an angle of 170°, were arranged in a symmetrical-cone geometry as shown in Fig. 2. This arrangement helps to minimize the uncertainty due to beam misalignment causing angle offset and also helps to obtain good statistics in a short time. To check the consistency of the measured QE scattering events, one more telescope was placed at an angle of 140°. Two 300-μm-thick silicon detectors were placed at ±10° with respect to the beam direction, for beam monitoring and normalization purposes. The energy resolution of these detectors (less than 18 keV for 5.48 MeV α particles) is sufficient to separate the elastically scattered events and recoil events. The spectra obtained using the telescope detectors and the analysis performed to obtain the BD are reported in the following section.

B. QE excitation function and BD

The QE events are defined as the sum of the elastic, inelastic, and transfer events. So, the ΔE-E detector telescopes described above were employed for the identification of these scattering events. Figure 3 shows a typical two-dimensional correlation plot of ΔE-E (energy loss versus residual energy) obtained with $E_{\rm lab} = 118$ MeV at $\theta_{\rm lab} = 170^\circ$ for the ^{28}Si + ^{154}Sm system. The prominent lobe includes elastic, inelastic, and neutron-transfer events, which are indistinguishable. The various other lobes correspond to 1p, 2p, and 3p

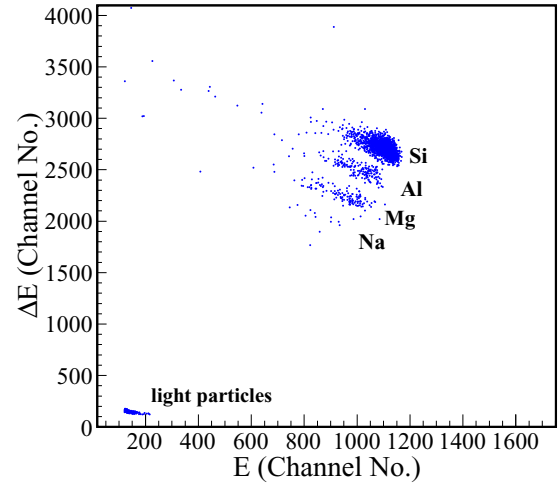

FIG. 3. Two-dimensional correlation plot of ΔE-E energy signals from the hybrid telescope detector at 170° with respect to the beam direction in the ^{28}Si + ^{154}Sm reaction at $E_{\rm lab} = 118$ MeV. Projectile-like fragments of different atomic numbers are identified.

stripping channels as shown in Fig. 3. Low statistics for 1p, 2p, and 3p channels can be attributed to negative Q values for these channel. The counts from all the lobes were summed to obtain the total QE events.

To check the consistency of the experimental data, the QE measurements were performed at two different backward angles, 170° and 140°. The results of QE events at 170° and 140° were converted to those for 180° by mapping to an effective energy $E_{\rm eff}$ using the relation [23]

$$E_{\rm eff} = \frac{2E_{\rm c.m.}}{1 + \mathrm{cosec}\left(\frac{\theta_{\rm c.m.}}{2}\right)}, \tag{1}$$

where $E_{\rm c.m.}$ and $\theta_{\rm c.m.}$ are the center-of-mass energy and scattering angle, respectively. Since in the semiclassical approximation, each scattering angle corresponds to scattering at a certain angular momentum, and the cross section can be scaled in energy by taking into account the centrifugal correction. Thus the mapping approximately corrects for angle-dependent centrifugal effects through $\sigma_{\rm qe}(E_{\rm eff},\pi) \approx \sigma_{\rm qe}(E_{\rm c.m.},\theta_{\rm c.m.})$. However, the mapping becomes less good for smaller scattering angles [25]. Also at smaller scattering angles, the elastic cross section will display Fresnel oscillations, which will cause the derived distribution to oscillate [25]. Hence, the detector angles were chosen as $\theta_{\rm lab} = 170^\circ$ and 140° in the present work. The QE cross sections $\sigma_{\rm qe}(E_{\rm eff},\pi)$, normalized to the Rutherford cross section, that is, $(d\sigma_{\rm qe}/d\sigma_{\rm R})(E,\pi)$, are shown in Fig. 4(a) for our two detector angles $\theta_{\rm lab} = 170^\circ$ and 140°. It can be seen from Fig. 4(a) that the QE excitation functions obtained from these two angles overlap extremely well with one another. The statistical error is found to be less than 1% at the lower energies and around 2% at higher energies.

In a classical picture, projectiles incident on a target can either get scattered or get captured. Since capture is related to the transmission through the barrier for $l = 0$, whereas large-angle QE scattering is related to reflection at the same barrier, these two processes are complementary to each other.

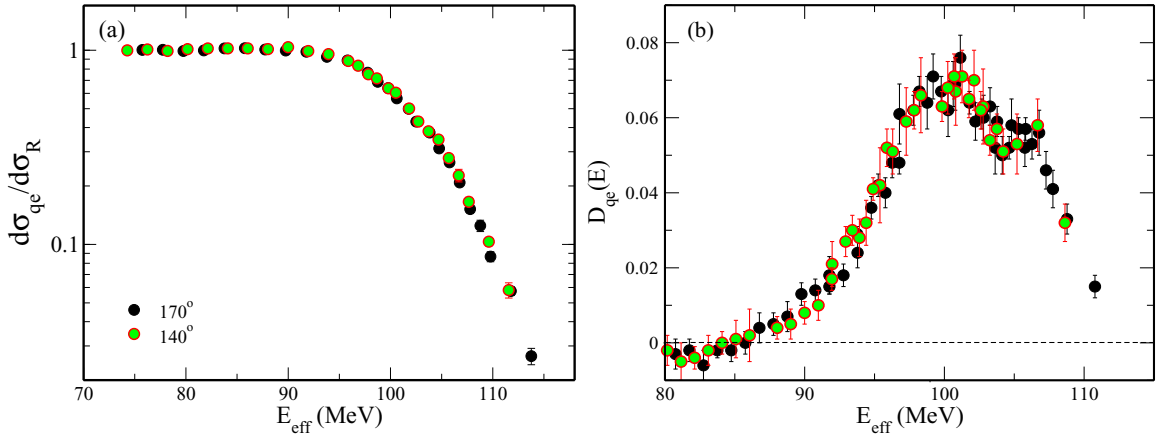

FIG. 4. (a) Quasi-elastic excitation function and (b) corresponding barrier distribution obtained at two backward scattering angles, $\theta_{\rm lab} = 170^\circ$ and 140°, for the ^{28}Si + ^{154}Sm system.

Here, however, processes like deep inelastic collision and noncompound fission are negligible. Hence, capture cross section is expected to be very close to fusion cross section. Moreover, the reflection coefficient R_0 for angular momentum $l = 0$ is approximately equal to the ratio $(d\sigma_{\rm qe}/d\sigma_{\rm R})(E)$ at $\theta = \pi$. The transmission coefficient T_0 is related to the reflection coefficient by $T_0 = 1 - R_0$ and it implies that $dT_0/dE = -dR_0/dE$. Since the fusion BD, $D_{\rm fus}(E)$, is described as $D_{\rm fus}(E) = dT_0/dE = d^2(E\sigma_{\rm fus})/dE^2$, it then follows that [25]

$$D_{\rm qe}(E_{\rm eff},\theta) = -\frac{dR_0}{dE}(E_{\rm eff},\pi) = -\frac{d}{dE_{\rm eff}}\left[\frac{d\sigma_{\rm qe}(E_{\rm eff},\pi)}{d\sigma_{\rm R}(E_{\rm eff},\pi)}\right], \tag{2}$$

where $D_{\rm qe}(E_{\rm eff},\theta)$ represents the QE BD obtained from data taken at the scattering angle θ. The experimental BD was extracted from the QE excitation function using Eq. (2). As the QE excitation function is measured at two different angles, the corresponding BDs are compared in Fig. 4(b). The identical structure from QE measurements at two different angles gives us confidence in the consistency of our experimental data.

IV. RESULTS AND DISCUSSION

From the measured QE excitation function [Fig. 4(a)] it is apparent that the experimental average barrier for the ^{28}Si + ^{154}Sm system is almost same as that of its Bass barrier ($\approx$102 MeV). Here the average barrier is considered as the energy where the experimental QE excitation function is reduced to a value of 0.5. With precise QE data for ^{28}Si + ^{154}Sm, we can pursue further the experimental signature of coupling by comparing the measured data with those of the ^{16}O + ^{154}Sm system taken from Ref. [23]. With QE data for these two systems, we can follow the same scaling procedures performed on the fusion data in Sec. II.

A. Comparison of experimental QE data

Figures 5(a) and 5(b) show a comparison of the experimental QE excitation functions and BDs, respectively, for the two systems. The energy is shifted to account for the difference in barrier heights. As for the fusion data, the higher Z for ^{28}Si increases the width of the BD. Therefore, the ^{16}O data are scaled to remove this effect, so that any remaining differences should be simply due to the couplings effect in ^{28}Si, which may help to understand the realistic coupling scheme for ^{28}Si. The effect of the high-energy octupole excitation in ^{16}O is removed by shifting the data. (Note, however, that the displacement now required is 2.0 MeV, which is 0.5 MeV greater than observed in the fusion data. This may be due to incident energy straggling and/or unknown homogeneities in the target.) Figure 5(c) shows the resulting QE excitation function after these operations are performed on the ^{16}O data. For energies below the barrier, the QE excitation functions appear to be identical. However, at the highest energies [$(E_{\rm eff} - V_{\rm B}) > 5$ MeV], the slope of the function appears to be different for the two systems. In other words, the QE cross section for ^{28}Si + ^{154}Sm shows an enhancement compared with that for ^{16}O + ^{154}Sm system at the highest energies.

To better visualize the difference we compare the two experimental QE BDs in Fig. 5(d). This reveals an interesting feature for the ^{28}Si + ^{154}Sm system. A peaklike structure shown by the arrow in Fig. 5(d) is clearly visible for this system and is absent for ^{16}O + ^{154}Sm. Since all other effects are essentially eliminated, we can attribute this structure to couplings to ^{28}Si excitations.

B. Coupled-channels calculations

In order to explain the obtained QE data, the coupled-channels calculations with different target-projectile coupling schemes were performed using a scattering version of the CCFULL program [1]. The program provides the QE excitation functions from which our theoretical BDs were extracted using the method described in Ref. [25]. In the program, the nuclear potential has real and imaginary components, both of which are assumed to have a Woods-Saxon form. The imaginary part simulates compound nucleus processes, and we have used a depth parameter of 30 MeV, radius parameter of 1.0 fm, and surface diffuseness parameter of 0.3 fm. This choice of parameters confines the imaginary potential inside

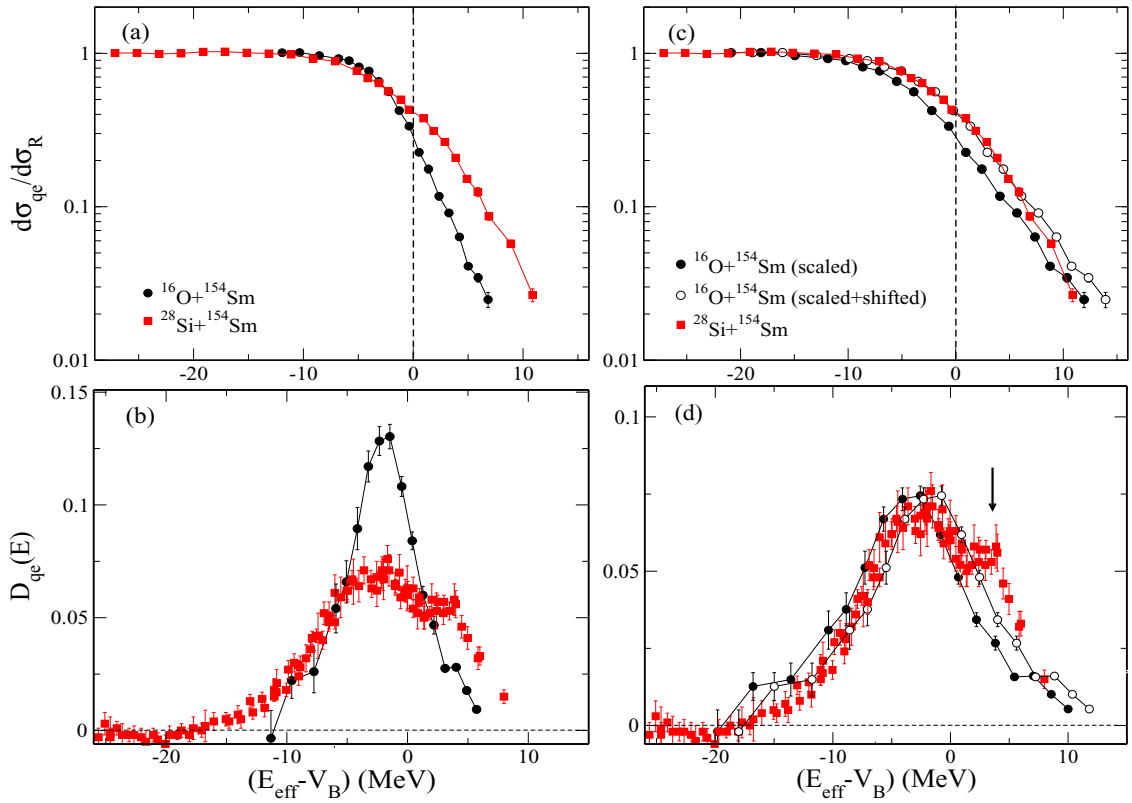

FIG. 5. Comparison of experimental QE excitation functions (upper panels) and corresponding barrier distributions (lower panels) for the systems $^{16}O + ^{154}Sm$ and $^{28}Si + ^{154}Sm$. Left-hand plots (a) and (b) are before scaling whereas right-hand plots (c) and (d) show the comparison after scaling the $^{16}O + ^{154}Sm$ data and after applying a small extra shift (see text). The vertical dashed lines in panels (a) and (b) correspond to the position of the Bass barrier.

the Coulomb barrier with a negligible strength in the surface region. As long as the imaginary potential is confined inside the Coulomb barrier with sufficiently large strength, the results are insensitive to details of its parameters. For the real part of the nuclear potential, the depth V_0 is fixed to be 185 MeV. We have fixed the value of V_0 because the effect of variation in V_0 and r_0 on the Coulomb barrier height compensates for each other in the surface region. That is, for a given value of diffuseness parameter, the results do not significantly depend upon the actual choice of V_0, as long as the same barrier height is maintained. Taking a reasonable value of $a = 0.65$ fm for the surface diffuseness parameter, the radius parameter r_0 is adjusted such that the barrier height without coupling is same as the Bass barrier [24]. We ultimately find a value of $r_0 = 1.11$ fm, which yields an uncoupled barrier height of 102.23 MeV, very close to the Bass value of 102.90 MeV.

Figures 6(a) and 6(b) show the theoretical excitation functions and BDs, respectively, along with the corresponding experimental data. It can be seen that theory does not reproduce the experimental data when no couplings are included (dashed line). The inclusion of lower members of the rotational band of ^{154}Sm considerably improves the fit but the calculations essentially converge after inclusion of the 2^+, 4^+, and 6^+ states, with results that still fall short of the experimental data. Thus, we can conclude that coupling to excited states of the ^{28}Si projectile cannot be ignored. Our calculations show that when the rotational coupling to the target alone is included, considering the projectile to be inert, the most probable barrier shifts by ≈2 MeV above the uncoupled barrier.

To understand the coupling of ^{28}Si, we tried the rotational as well as vibrational model estimates since its excited-state energies do not correspond to any of these models. Hence, the coupled-channel calculations were performed including the 2^+ state of ^{28}Si along with the rotational states of ^{154}Sm. The various coupling parameters used are given in Table I. The value $\beta_4 = 0.10$ for the ^{28}Si hexadecapole deformation parameter was reported in a recent paper [11], and was used in our initial calculations in Fig. 6. It is clear from the figure that although the excitation function looks quite similar for two different excitations of ^{28}Si, the more sensitive BD (taken using 2 MeV steps) shows significant differences between the vibrational and rotational coupling schemes. It appears from Fig. 6(b) that the high-energy side of the BD is better fitted by vibrational coupling rather than by the expected rotational coupling to 2^+ state. Such an observation is in contrast with

TABLE I. Coupling parameters used in the calculations. All energies are in MeV.

Nucleus	E_{2^+}	β_2	β_4	E_{3^-}	β_3
^{28}Si	1.779	−0.407	0.10 [11] 0.25 [26]		
^{154}Sm	0.081	0.341	0.07	1.012	0.142

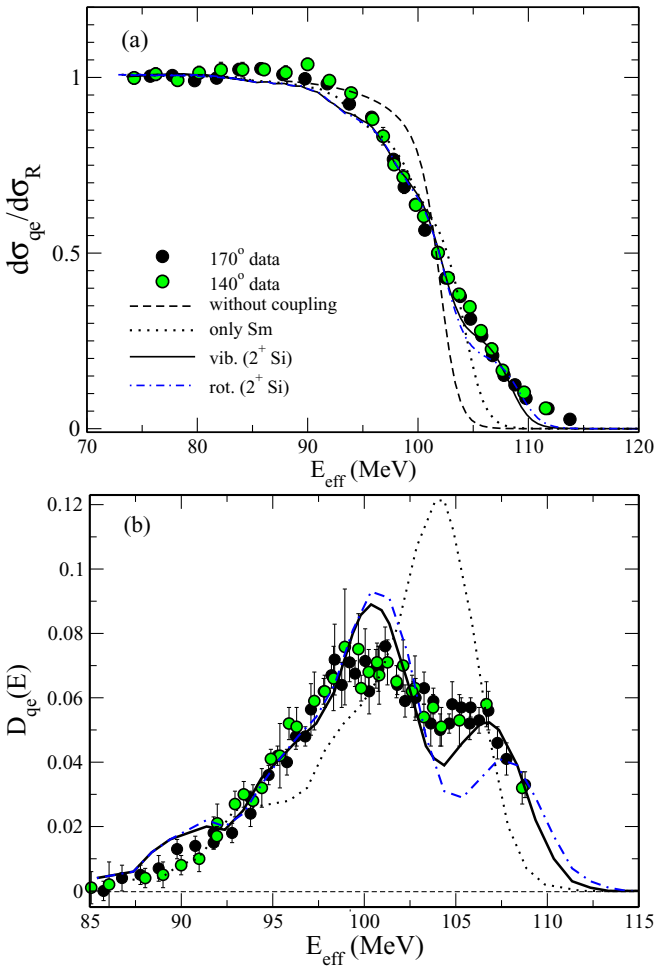

FIG. 6. (a) Coupled-channels predictions compared with experimental QE excitation functions and (b) the resulting barrier distributions for the ^{28}Si + ^{154}Sm system. The plot shows results obtained with vibrational (solid line) and rotational (dotted-dash line) couplings for the first 2^+ state of ^{28}Si; the rotational calculation takes $\beta_4 = 0.1$.

previous studies for the fusion of ^{28}Si with spherical and near-spherical targets [5–11], where rotational couplings seem to explain the experimental data (or excitation function) better.

However, the only qualitative difference between the rotational and vibrational coupling schemes is the absence of a reorientation term when the 2^+ state is treated as a phonon. That is, there is no $2_1^+ \rightarrow 2_1^+$ coupling. In the rotational scheme, this coupling is present and it is important here to note that the 2^+ state may be coupled to itself by both quadrupole and hexadecapole deformations. The coupling strength will, therefore, depend on the value of β_4 that one uses. There is a range of positive values of this parameter in the literature, though most rather larger than the value used above. The best theoretical value is probably that due to Möller and Nix [26], $\beta_4 = 0.25$. When we repeat our calculations using this value we see (Fig. 7) that the new rotational results are barely different from those for the vibrational calculation. In other words, the hexadecapole contribution to the reorientation coupling practically cancels out the quadrupole contribution.

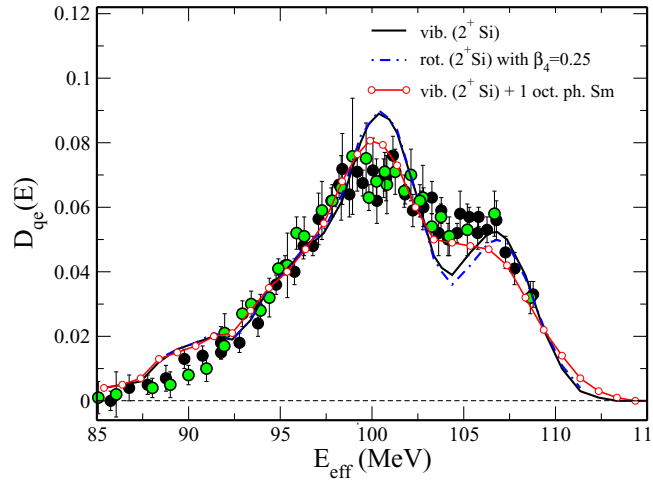

FIG. 7. Same as Fig. 6, but with the larger value of $\beta_4 = 0.25$ in the rotational coupling. Note the smoothing introduced by inclusion of the ^{154}Sm octupole vibration.

Apart from this, we observe that the effect of negative value of hexadecapole deformation ($\beta_4 = -0.25$) of the ^{28}Si. It causes the shift in the high-energy peak of the BD by ≈3 MeV towards higher energy side with respect to that for its positive value and gives poor representation of the experimental BD (not shown here). Hence, this shows the value of β_4 for ^{28}Si to be positive.

We note that the remaining major difference between the theoretical calculation and the data is that the experimental structure is smoother. The only other significant collective state in this system is the 3^- octupole state of ^{154}Sm and we find in Fig. 7 that its inclusion in our calculations does indeed smear the theoretical BD to give a final result in better agreement with the data. (Though note that coupling to many weak, direct inelastic channels can also contribute to smoothing of the distribution; see, for example, Refs. [27,28].) Until now, we have discussed only the 2^+ state of ^{28}Si; however, inclusion of its 4^+ state in coupled-channel calculations merely shifts the relative position of the peak and shoulder in the BD by around 0.6 MeV toward the lower energy side with no significant changes in their heights; it does not therefore influence the present conclusions.

V. SUMMARY AND CONCLUSION

We have discussed the influence of couplings to excited states of ^{28}Si projectile and ^{154}Sm target on fusion through BD studies. The BD was obtained through QE scattering experiment at large backward angles. We tried to understand the coupling not only by theoretical means (i.e., through coupled-channel calculations) but also by locating the effect of the coupling in the experimentally observed BD. To this end, the experimental signatures of ^{154}Sm and ^{28}Si are explored by comparing the QE excitation function and corresponding BD of the ^{28}Si + ^{154}Sm system with those for ^{16}O + ^{154}Sm. The strong similarity between their BD showed that the ^{154}Sm deformation plays a dominating role in the fusion process. Furthermore, it has been observed that the

effect of collective state excitation in ^{28}Si has been reflected as a peaklike structure on the higher energy side of the BD.

On the theoretical front, it is observed that the peaklike structure of ^{28}Si could be reproduced using coupled-channel calculations as a pure vibrator despite its well-established rotational nature. The resolution of this anomaly lies in the hexadecapole deformation of ^{28}Si; the contributions to the reorientation coupling ($2_1^+ \rightarrow 2_1^+$) from the quadrupole deformation is largely canceled out by that from the hexadecapole deformation. In order to achieve this cancellation, one requires a large positive value of β_4 and we have used here the Möller-Nix value of $\beta_4 = 0.25$ [26], a value also obtained from proton scattering experiments [13]. Although our results cannot be regarded as a measurement of this quantity, we believe that they do at least confirm that this nucleus does indeed possess a large positive hexadecapole moment. Recently, the hexadecapole deformation of target nuclei is estimated from QE scattering experimental technique [19]. To the best of our knowledge, for the first time we observe the sensitivity of hexadecapole deformation of projectile on the BD extracted from QE experimental technique.

Moreover, in our theoretical calculations, we have observed that when deformation of ^{154}Sm is included alone, considering the projectile to be inert, the most probable barrier shifts by $\approx$2 MeV above the uncoupled barrier. This may have implications in the heavier systems where deformed actinide targets are utilized for the production of SHEs. Such a shift in the most probable barrier (deciding the probability of SHE formation) may occur when the deformed target interacts either with spherical projectile or if the projectile excitation is weaker relative to permanent deformation of the target.

Even though the target considered here is permanently deformed with significantly large coupling influence on BD, the experimental observation as well as coupled-channels calculations suggest that the QE BD (hence fusion) is sensitive to projectile excitations. Moreover, we may expect the sensitivity to be more pronounced with the spherical targets having small coupling effect on BD relative to that for deformed targets. It is hoped that these QE reactions may offer an alternative method of identifying the coupling to excitation in other projectiles. Hence for heavier systems where the compound nucleus is too fissile, one can attempt to study the coupling effects by measuring QE scattering. Currently, a variety of analyses, aimed at identifying the coupling effects of various degrees of freedom on the synthesis of SHEs, are being carried out. It is apparent from our results that care must be taken in such analyses, especially for systems populating SHEs where projectiles such as ^{28}Si and ^{48}Ti are used on actinide targets. Considering their excitations as purely rotational or vibrational may lead to an incorrect interpretation of the fusion probability and additional degrees of freedom may be wrongly assumed to play a role. Therefore, more sophisticated analysis, such as use of a coupling potential constructed by microscopic nuclear structure calculation (instead of employing the macroscopic vibrational or rotational model) is desirable to reach a fair understanding in future.

ACKNOWLEDGMENTS

We are grateful to the Pelletron staff of the IUAC for providing a stable and good current beam throughout the experiment. The help and support received from Rajeev Ahuja and the workshop staff during the detector fabrication are highly acknowledged. One of the authors, G.K., gratefully acknowledges the University Grants Commission (UGC), New Delhi, for providing the financial support for this work. Part of this work was carried out with the DST PURSE grant of Panjab University, Chandigarh.

[1] K. Hagino, N. Rowley, and A. T. Kruppa, Comput. Phys. Commun. **123**, 143 (1999).
[2] K. Hagino and N. Takigawa, Prog. Theor. Phys. **128**, 1061 (2012).
[3] M. Dasgupta, D. J. Hinde, N. Rowley, and A. M. Stefanini, Annu. Rev. Nucl. Part. Sci. **48**, 401 (1998).
[4] K. Hagino and J. M. Yao, Phys. Rev. C **91**, 064606 (2015).
[5] J. O. Newton, C. R. Morton, M. Dasgupta, J. R. Leigh, J. C. Mein, D. J. Hinde, H. Timmers, and K. Hagino, Phys. Rev. C **64**, 064608 (2001).
[6] S. Kalkal, S. Mandal, N. Madhavan, E. Prasad, S. Verma, A. Jhingan, R. Sandal, S. Nath, J. Gehlot, B. R. Behera, M. Saxena, S. Goyal, D. Siwal, R. Garg, U. D. Pramanik, S. Kumar, T. Varughese, K. S. Golda, S. Muralithar, A. K. Sinha, and R. Singh, Phys. Rev. C **81**, 044610 (2010).
[7] M. Dasgupta, A. Navin, Y. K. Agarwal, C. V. K. Baba, H. C. Jain, M. L. Jhingan, and A. Roy, Nucl. Phys. A **539**, 351 (1992).
[8] D. Ackermann, F. Scarlassara, P. Bednarczyk, S. Beghini, L. Corradi, G. Montagnoli, L. Müller, D. R. Napoli, C. M. Petrache, K. M. Varier, F. Soramel, P. Spolaore, A. M. Stefanini, G. F. Segato, C. Signorini, and H. Zhang, Nucl. Phys. A **583**, 129 (1995).
[9] B. K. Nayak, R. K. Choudhury, A. Saxena, P. K. Sahu, R. G. Thomas, D. C. Biswas, B. V. John, E. T. Mirgule, Y. K. Gupta, M. Bhike, and H. G. Rajprakash, Phys. Rev. C **75**, 054615 (2007).
[10] L. T. Baby, V. Tripathi, J. J. Das, P. Sugathan, N. Madhavan, A. K. Sinha, M. C. Radhakrishna, P. V. Madhusudhana Rao, S. K. Hui, and K. Hagino, Phys. Rev. C **62**, 014603 (2000).
[11] L. S. Danu, B. K. Nayak, E. T. Mirgule, R. K. Choudhury, and U. Garg, Phys. Rev. C **89**, 044607 (2014).
[12] Y. Horikawa, Prog. Theor. Phys. **47**, 867 (1972); Y. Horikawa, A. Nakada, and Y. Torizuka, *ibid.* **49**, 2005 (1973).
[13] R. de Swiniarski, C. Glashausser, D. L. Hendrie, J. Sherman, A. D. Bacher, and E. A. McClatchie, Phys. Rev. Lett. **23**, 317 (1969).
[14] C. R. Howell, R. S. Pedroni, G. M. Honoré, K. Murphy, R. C. Byrd, G. Tungate, and R. L. Walter, Phys. Rev. C **38**, 1552 (1988).
[15] H. Rebel, G. W. Schweimer, J. Specht, and G. Schatz, R. Löhken, D. Habs, G. Hauser, and H. Klewe-Nebenius, Phys. Rev. Lett. **26**, 1190 (1971).
[16] J. X. Wei, J. R. Leigh, D. J. Hinde, J. O. Newton, R. C. Lemmon, S. Elfstrom, J. X. Chen, and N. Rowley, Phys. Rev. Lett. **67**, 3368 (1991).

[17] J. R. Leigh, N. Rowley, R. C. Lemmon, D. J. Hinde, J. O. Newton, J. X. Wei, J. C. Mein, C. R. Morton, S. Kuyucak, and A. T. Kruppa, Phys. Rev. C **47**, R437 (1993).
[18] J. R. Leigh, M. Dasgupta, D. J. Hinde, J. C. Mein, C. R. Morton, R. C. Lemmon, J. P. Lestone, J. O. Newton, H. Timmers, J. X. Wei, and N. Rowley, Phys. Rev. C **52**, 3151 (1995).
[19] H. M. Jia, C. J. Lin, F. Yang, X. X. Xu, H. Q. Zhang, Z. H. Liu, Z. D. Wu, L. Yang, N. R. Ma, P. F. Bao, and L. J. Sun, Phys. Rev. C **90**, 031601(R) (2014).
[20] S. Gil, D. Abriola, D. E. DiGregorio, M. di Tada, M. Elgue, A. Etchegoyen, M. C. Etchegoyen, J. Fernández Niello, A. M. J. Ferrero, A. O. Macchiavelli, A. J. Pacheco, J. E. Testoni, P. Silveira Gomes, V. R. Vanin, A. Charlop, A. García, S. Kailas, S. J. Luke, E. Renshaw, and R. Vandenbosch, Phys. Rev. Lett. **65**, 3100 (1990).
[21] B. Castel and J. C. Parikh, Phys. Rev. C **1**, 990 (1970).
[22] K. Hagino, N. Takigawa, M. Dasgupta, D. J. Hinde, and J. R. Leigh, Phys. Rev. Lett. **79**, 2014 (1997).
[23] H. Timmers, J. R. Leigh, M. Dasgupta, D. J. Hinde, R. C. Lemmon, J. C. Mein, C. R. Morton, J. O. Newton, and N. Rowley, Nucl. Phys. A **584**, 190 (1995).
[24] R. Bass, Phys. Rev. Lett. **39**, 265 (1977).
[25] K. Hagino and N. Rowley, Phys. Rev. C **69**, 054610 (2004).
[26] P. Möller and J. R. Nix, At. Data Nucl. Data Tables **59**, 185 (1995).
[27] S. Yusa, K. Hagino, and N. Rowley, Phys. Rev. C **88**, 044620 (2013).
[28] E. Piasecki, Ł. Świderski, W. Gawlikowicz, J. Jastrzębski, N. Keeley, M. Kisieliński, S. Kliczewski, A. Kordyasz, M. Kowalczyk, S. Khlebnikov, E. Koshchiy, E. Kozulin, T. Krogulski, T. Loktev, M. Mutterer, K. Piasecki, A. Piórkowska, K. Rusek, A. Staudt, M. Sillanpää, S. Smirnov, I. Strojek, G. Tiourin, W. H. Trzaska, A. Trzcińska, K. Hagino, and N. Rowley, Phys. Rev. C **80**, 054613 (2009).